

A Statistical Analysis of Hadron Spectrum :

Quantum Chaos in Hadrons

Vladimir Pascalutsa

The School of Chemistry,

Physics and Earth Sciences,

Flinn University,

Bedford Park, SA 5042, Australia

and

Department of Physics and Astronomy,

Ohio University, Athens, OH 45701^y

(Dated: January 30, 2020)

Abstract

The nearest-neighbor mass-spacing distribution of the measured meson and baryon spectrum (up to 2.5 GeV) is described by the Wigner sum rule corresponding to the statistics of the Gaussian orthogonal ensemble of random matrix theory. This can be viewed as a manifestation of quantum chaos in hadronic systems.

PACS numbers: 05.45.Mt, 14.20.-c, 14.40.-n

Electronic address: vlad@phy.ohio.edu

^yPresent address.

Quarks are glued into colorless objects called hadrons, forming a large and complex hadron spectrum. Understanding this spectrum is a direct way to learn about quark-gluon interactions in the constituent regime, and therefore hadron spectroscopy is a very active field of research both theoretically and experimentally. In the study of complex spectra, in general, statistical methods have proved to be useful. One of the early successes of statistical analysis was Wigner's celebrated discovery of the fact that statistical properties of complex nuclear spectra are described by the Random Matrix Theory (RMT) [1, 2, 3, 4]. It was later realized that these properties, referred to as Wigner-Dyson properties, have a great deal of universality and appear in spectra of many physical systems, ranging from quantum dots [5] to lattice gauge theories [6, 7, 8].

In this Letter we show that the experimentally measured hadron spectrum has at least some Wigner-Dyson properties as well. Once this is established the link to the underlying dynamics can made via the Bohigas-Giannoni-Schmit (BGS) conjecture [9] which claims that the Wigner-Dyson properties are generic to spectra of the systems with a quantum analog of chaotic dynamics | so called quantum chaos (see, e.g., [10, 11]).

Recent theoretical work in lattice QCD [6, 7] and quantum-mechanical Yang-Mills models [8, 12] already addresses the statistical properties of QCD spectrum as well as the quantum chaos aspects. Our findings will provide certain empirical support of these results and, hopefully, motivate further studies in this direction.

We look at the experimental hadron spectrum as is compiled by the Particle Data Group (PDG). We shall be concerned only with the fluctuation properties of the mass-splitting (level spacing) between hadrons with the same set of good quantum numbers (QNs). In the analysis we include the non-strange and strange hadrons from the PDG Summary Tables [13]. More specifically, we have taken [14]: N_c , π , ρ , and baryons up to N_c (2200), excluding the one-star baryons; and all the mesons listed in the Summary Tables up to f_2 (2340). We have thus truncated the spectrum at about 2.5 GeV, since the lower states are more reliably known.

Using these data we would like to examine the probability distribution of spacings, $S_i = m_{i+1} - m_i$, between nearest-neighbor hadrons with the same conserved QNs, namely: isospin, spin, parity, strangeness, baryon number, and, in case of mesons, charge conjugation. We first do it for baryons. The baryon spectrum is thus subdivided into small multiplets, each characterized by a set of definite QNs. Each multiplet provides a number of spacings into

the common array of spacings $fs_i g_B$. The spacings are then scaled out: $fs_i g_B = fs_i = hS_i g_B$, by the mean spacing hS_i .

The same procedure is applied to the meson spectrum to obtain array $fs_i g_M$. It is important to note that the baryon and meson mean spacing come out to be very close, see Table I. This is why it makes sense to consider a combined array of hadron spacings: $fs_i g_H = fs_i g_B ; fs_i g_M$.

Spectrum	hS _i , in MeV	
Baryon	289.8	18.8
Meson	284.3	35.8
Combined	287.1	27.3

TABLE I: Mean mass spacing. The error bars stem from the PDG quoted errors.

Histograms of the resulting spacing distributions, $p(fs_i g_B)$, $p(fs_i g_M)$, and $p(fs_i g_H)$ are presented in the left panel of Fig. 1. The right panel of the figure presents the result of analysis done without distinguishing the QNs ("M fixed QNs"). The curves in the figure show the Poisson-like distribution [$p(s) = \exp(-s)$], and the Wigner sum rule [$p(s) = \frac{1}{2} s \exp(-\frac{1}{4}s^2)$]. They represent two extreme regimes: uncorrelated spectrum (Poisson) vs. a strongly correlated one (Wigner-Dyson).

The figure shows that while for fixed QNs the experimental spectrum is uncorrelated, in the case of states with equal QNs there is a strong correlation (in fact, repulsion) of the states. Very similar picture occurs in the nuclear spectra [15], and, as is already mentioned, the situation appears to be generic to systems whose classical counterpart is essentially chaotic.

The histogram plots represent the empirical distributions in a rather qualitative view because the statistics is low and hence the picture is sensitive to the choice of the grid. Accounting for the error bars makes it even less accurate. More precise and instructive characteristics are the moments of a distribution. For our empirical distribution the n-th moment is simply calculated as

$$hS^n i_{\text{exp}} = \frac{1}{N} \sum_{i=1}^N s_i^n; \quad (1)$$

which obviously is insensitive to the above mentioned artifacts of the analysis.

At the same time let us consider a more general form of the Wigner sum is:

$$p_W(s) = A s \exp(-B s^2) \quad (2)$$

where β is a parameter | the Dyson index; A and B are constants fixed by the normalization conditions: $\int_{-\infty}^{\infty} p_W(s) ds = 1 = \int_{-\infty}^{\infty} s^2 p_W(s) ds$, where, naturally, $\int_{-\infty}^{\infty} s^n p_W(s) ds = \frac{1}{n+1} \int_{-\infty}^{\infty} s^{n+1} p_W(s) ds$. Depending on the value of β expression (2) approximates the spacing distributions of the RMT for various types of Gaussian ensembles. The most common values are $\beta = 1, 2$, and 4 which represent the orthogonal (GOE), unitary (GUE), and symplectic (GSE) ensembles, respectively.

Computing the first ten, or so, moments of all the relevant distributions we obtain Figure 2. The moments of the Poisson distribution (shown by dashed lines) are given by the Gamma-function $\int_{-\infty}^{\infty} s^n p_{\text{Poisson}}(s) ds = (n+1)!$. The other curves represent the moments of the Wigner sum is for $\beta = 1, 2$, and 4 , respectively. They are also proportional to the Gamma-function [e.g., for $\beta = 1$, $\int_{-\infty}^{\infty} s^n p_W(s) ds = (2e^{-\frac{B}{2}})^n \Gamma(\frac{1}{2}n+1)$], and so all increase rapidly with n .

Data points in the first three panels correspond to the empirical distributions shown by the histograms in the left panel of Fig. 1, now with the PDG error bars properly accounted for [19]. It indeed turns out they all nicely agree with the Wigner sum is for $\beta = 1$. The χ^2 -point values are $0.47, 0.60, 0.52$ for the baryon, meson, and combined data, respectively.

Data points in the forth panel present the result of our RMT Monte-Carlo simulation using a sample of 10^4 of 4×4 random matrices from the GOE. It demonstrates the extent to which the Wigner sum is is a good approximation of the RMT distributions.

The quality of the hadron data, although not being excellent, apparently allows us to claim that fluctuation properties of the hadron spectrum fall into the GOE ($\beta = 1$) universality class, characterized by good time-reversal and rotational symmetry. This finding should play an important role in hadron spectroscopy, since it may constraint the theoretical modeling. For instance, in lattice simulations depending on approach one obtains the Dirac spectra that to different universality classes [16], although it should be noted that Dirac spectra relate to the hadron spectrum only after averaging over the gauge fields.

Quark models presently are further away from addressing the statistical properties of the spectrum. Of course the model that reproduces the physical spectrum well enough should inevitably have the same statistical properties. It may thus be interesting to see whether the quark-model Hamiltonians that the spectrum indeed define a chaotic classical system, as is inferred by the BGS conjecture.

Finally, if hadrons indeed have these universal statistical properties, the hadron-exchange models (e.g.[17]) should be able benefit from the RMT methods, in a way analogous to the stochastic theory of compound-nucleus reactions [4, 18]. However, since unitarity is an essential ingredient of such models, a study of hadron width distribution is in order. Widths of compound nuclei have the Porter-Thomas distribution [3] that eventually allows one to define the unitary S-matrix completely within the RMT. We anticipate that the same approach will be applicable in the hadron-exchange reactions once the hadron-width distribution is determined.

In conclusion, we have examined the nearest-neighbor level-spacing (mass-splitting) distribution of the experimental hadron spectrum. The mean level-spacing seems to be the only relevant scale here, and after it is scaled out the distribution shows universal behavior. Unfortunately, the masses and quantum numbers are well known only for a few dozen hadron states, so achieving high statistics is out of the question. Nonetheless, the low-statistics analysis we have performed pinpoints the moments of the distribution accurately enough to claim that hadron spectrum falls into the same universality class as random matrices from the GOE. Invoking the BGS conjecture, we view our result as an empirical evidence for the "quantum chaos" phenomenon in hadrons.

Acknowledgments

I thank Professor Iraj Afan for valuable discussions, and Professors Daniel Phillips and Jac Verbaarschot for critical remarks on the manuscript. The work was supported by the Australian Research Council (ARC) and in part by DOE under grant DE-FG 02-93ER 40756.

[1] E.P. Wigner, *Ann. Math.* 53, 36 (1951); 62, 548 (1955); 65, 203 (1957); 67, 325 (1958).

[2] F.J. Dyson, *J. Math. Phys.* 3, 140 (1962); 3, 157 (1962); 3, 166 (1962); 3, 1199 (1962).

[3] C.E. Porter, *Statistical Theory of Spectra: Fluctuations* (Academic, New York, 1965), and references therein.

[4] T.A. Brody, J.F. Flores, J.B. French, P.A. Mello, A. Pandey and S.S. Wong, *Rev. Mod. Phys.* 53, 385 (1981).

[5] Y. Alhassid, *Rev. Mod. Phys.* 72, 895 (2000).

[6] M .A .Halasz and J. J.M .Verbaarschot, Phys. Rev. Lett. 74, 3920 (1995); D .Toublan and J.J.M .Verbaarschot, Nucl. Phys. B 603, 343 (2001).

[7] B .A .B erg, E .B ittner, H .M arkum , R .P ullirsch, M .P .Lombardo and T .W ettig, "U niversality and chaos in quantum field theories," arX iv:hep-lat/0007008.

[8] E .B ittner, H .M arkum and R .P ullirsch, Q uantum chaos in physical systems: From superconductors to quarks," arX iv:hep-lat/0110222.

[9] O .Bohigas, M .J .G iannoni and C .S chmit, Phys. Rev. Lett. 52, 1 (1984).

[10] M .C .G utzw iller, Chaos in Classical and Quantum Mechanics (Springer, Berlin, 1990).

[11] G .C asati and B .V .C hirikov, Quantum Chaos (Cambridge U .P ., Cambridge, 1995).

[12] L .S alasnich, Mod. Phys. Lett. A 12, 1473 (1997).

[13] D .E .G room et. al, Eur. Phys. J. C 15 1 (2000) [URL: <http://pdg.lbl.gov>].

[14] The precise database and Java codes used for the analysis are available from the author upon request.

[15] R .J .H aq, A .P andey, and O .Bohigas, Phys. Rev. Lett. 48, 1086 (1982).

[16] J .J .Verbaarschot, Nucl. Phys. Proc. Suppl. 90, 219 (2000).

[17] V .P ascalutsa and J .A .Tjon, Phys. Rev. C 61, 054003 (2000); V .P ascalutsa, Hadronic J. Suppl. 16, 1 (2001).

[18] J .J .Verbaarschot, H .A .W eidenm uller and M .R .Z imbauer, Phys. Rept. 129, 367 (1985).

[19] We account only for the the quoted mass-position error; the width is not viewed as one.

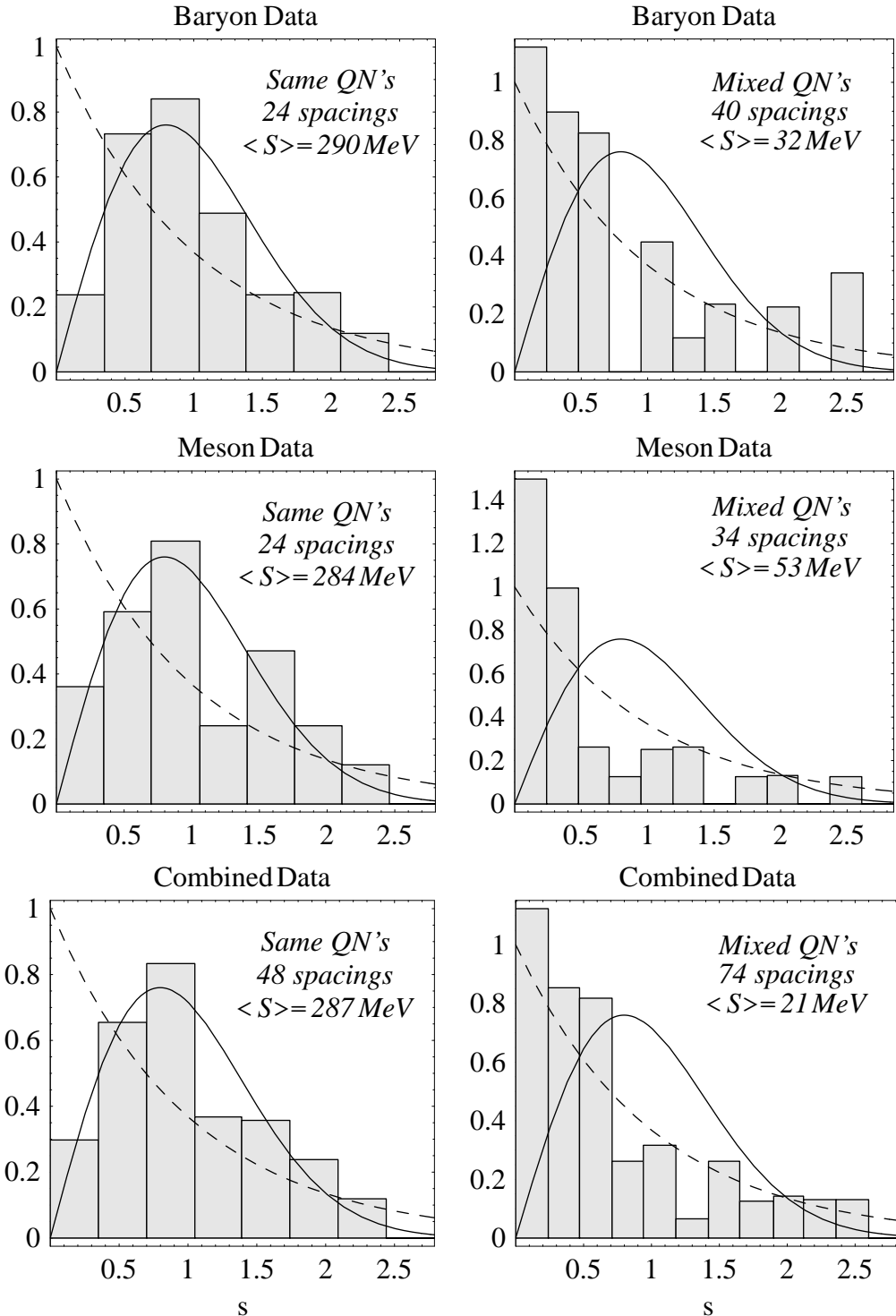


FIG. 1: Histograms of the nearest-neighbor mass spacing distribution for hadron states. Left panel { distributions of spacing between states of same QN's, right panel { mixed QN's. Curves represent the Poisson (dashed) and Wigner (solid) distributions, see text.

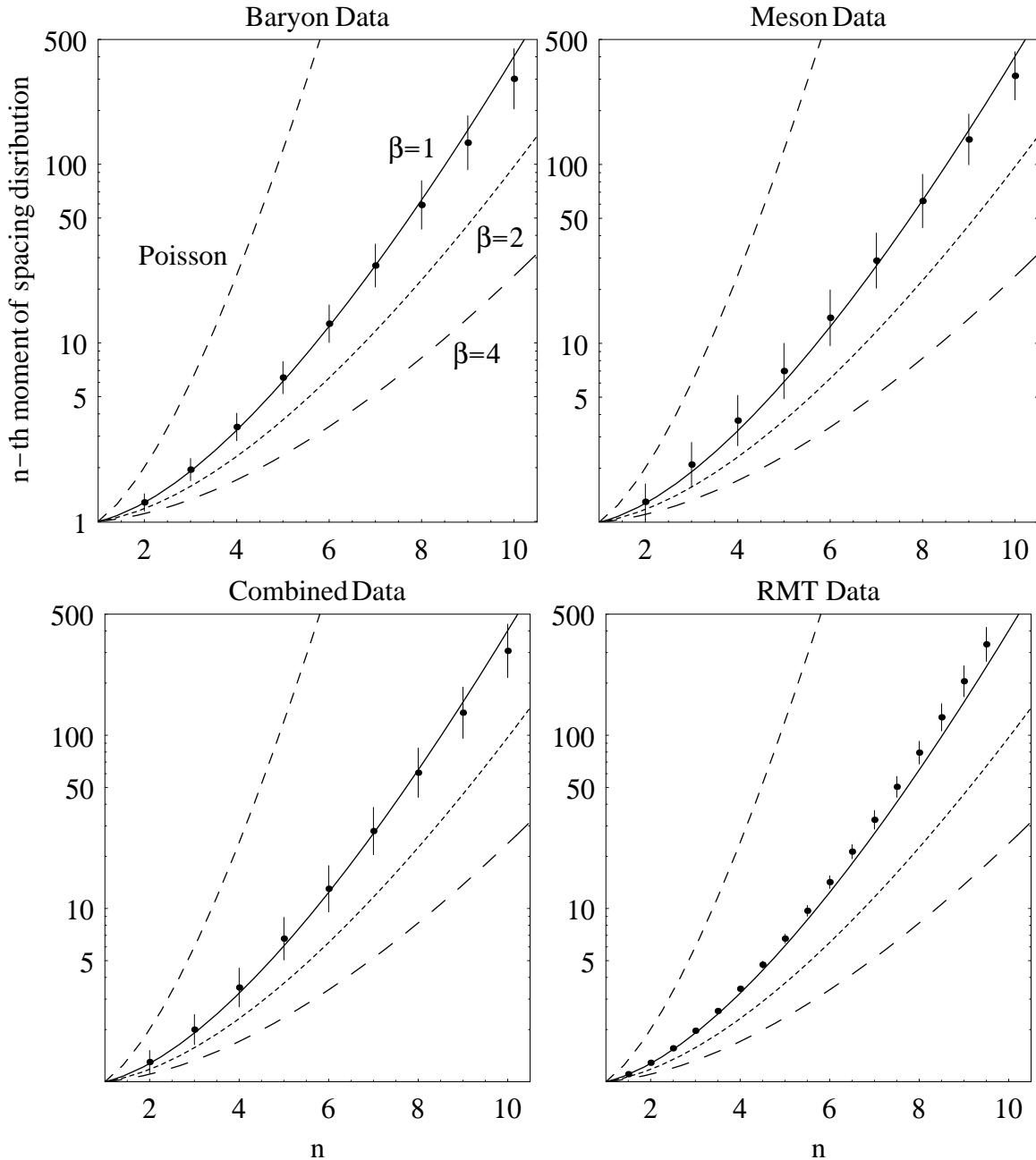


FIG. 2: Moments of spacing distributions. Explanations on the data points are given in the text. Curves represent the moments of Poisson distribution (dashed), and of the Wigner surmise for GOE (solid), GUE (short-dashed), and GSE (long-dashed).